Tribology International 55 (2012) 108–118

Contents lists available at SciVerse ScienceDirect

Tribology International

journal homepage: www.elsevier.com/locate/triboint

The effect of longitudinal tangential vibrations on friction and driving forces in sliding motion

Paweł Gutowski *, Mariusz Leus

Mechanical Engineering Faculty, West Pomeranian University of Technology, Szczecin (Katedra Mechaniki i Podstaw Konstrukcji Maszyn, Zachodniopomorski Uniwersytet Technologiczny w Szczecinie), 70–310 Szczecin, Al. Piastów 19, Poland

ARTICLE INFO

Article history:
Received 30 December 2011
Received in revised form
18 May 2012
Accepted 22 May 2012
Available online 1 June 2012

Keywords:
Friction force
Friction models
Longitudinal tangential vibrations
Driving force reduction

ABSTRACT

The main purpose of the work has been to qualitatively and quantitatively analyse the influence of longitudinal tangential vibrations on friction and driving forces in a sliding motion. Computational models were developed and implemented in a combined Matlab-Simulink environment. Both the dynamic Dahl's and the Dupont's and classical Coulomb's friction models were used. The influence of vibration velocity amplitude on the friction force in the presence of tangential longitudinal vibrations and on reduction of the driving force in sliding motion was analysed. It revealed that the commonly accepted view that the reduction of the average friction force is a consequence of cyclic changes in the sign of the friction force vector, only when the amplitude of vibration velocity is greater than the sliding motion velocity, is erroneous. The phenomenon was also observed without any changes in the sign of friction force vector. The results of simulations were compared with experimental data obtained with the use of a test rig specifically designed for the work. The Dahl's friction model led to the best correlation.

1. Introduction

The influence of vibrations on the static friction force and on friction force in sliding motions is well known and has been theoretically analysed and practically utilised for decades. It has been determined through experiments and theoretical analyses that a strict two-sided mutual relationship exists between friction and vibration. On one hand, friction in an operating mechanical system may be the source of a vibration and predominantly undesirable e.g. stick-slip. On the other hand, the magnitude and characteristic of the friction forces can be substantially changed by imposing high frequency micro-vibrations onto the system.

The described phenomenon has been the subject of broader analyses for more than half a century. In 1952 Baker et al. [1] determined that under the influence of small-amplitude forced mechanical vibrations the coefficient of static friction in the system had been minimised to almost zero. In 1959 Fridman and Levesque [2] demonstrated experimentally that ultrasonic vibrations may also significantly reduce the friction force. Whilst conducting experiments with vibrations in the frequency range between 6 and 42 kHz, forced perpendicular to the contact surface, they showed that the static friction coefficient of dry contact was almost zero.

Rapid development in nanotechnology has led to friction phenomenon on both micro- and nano-scale contact areas to be reported. Such investigations have a particular relevance to commonly used micro- and nano-electromechanical scanning probe techniques (MEMS/NEMS) in which traditional lubricants can unfortunately not be used as they increase the magnitude of friction and adhesion forces.

Comprehensive reviews in this domain have been published by Urbakh et al. [3] and Gnecco et al. [4]. Hesjedal and Behme [5,6] demonstrated that utilising the Rayleigh surface acoustic waves it is possible, at sufficiently high amplitude, to attain a complete elimination of static friction at micro-contact. They determined that this effect originates just from the normal component of vibrations. Gnecco and Socoliuc demonstrated that at an atomic scale a significant decrease of the friction and adhesion forces can be achieved through electro-capacitative actuation [7,8] as well as mechanical vibrations [4] excited in the normal direction through the use of a piezoelectric element. Such effect is observed in both vacuum and ambient conditions.

In the case of sliding motion at the macro-scale the influence of vibrations normal to the contact surface was investigated by researchers such as Pohlman and Lehfeld [9], Godfrey [10], Hess and Soom [11], Tolstoj et al. [12], Budanov et al. [13] and recently,

* Corresponding author. Tel.: +48 91 449 47 61.
E-mail addresses: pawel.gutowski@zut.edu.pl (P. Gutowski), mariusz.leus@zut.edu.pl (M. Leus).

0301-679X/$ - see front matter © 2012 Elsevier Ltd. All rights reserved.
http://dx.doi.org/10.1016/j.triboint.2012.05.023

Grudziński and Kostek [14] and Qu et al. [15]. Pohlman and Lehfeld stated, however, that significantly greater influence on the friction force in sliding motion than vibrations normal to the contact surface have tangential vibrations. Effect of these vibrations on the level of friction forces reduction was the subject of Mitskevich's [16] investigation.

Later this topic was also investigated, amongst others, by Skare and Stahl [17], Katoh [18], Sase et al. [19,20], Mutuonga [21], Siegert and Ulmer [22,23], Kutomi et al. [24], and in the current century, by Littmann et al. [25–27], Kumar and Hutchings [28], Tsay and Tseng [29] and by the authors of this work, Gutowski and Leus [30–34] as well as Popov et al. [35] and the above cited Qu et al. [15]. The latter demonstrated experimentally that the extent of friction reduction (decreases in the friction coefficient) in sliding motion at the micro-scale, under the influence of ultrasonic vibrations, significantly depends on the atmospheric pressure. They found out that the friction coefficient decreases as the atmospheric pressure reduces. This effect was observed to be significantly more pronounced for normal than tangential vibrations.

Three major theories exist to describe mechanism responsible for reducing friction resistance, at macro-scale, in sliding motion in relation to the direction of applied vibrations. In the case of vibrations normal to the contact surface, reduction in the friction force is frequently explained via reduction in the coefficient of friction. Alternative explanations focus on increase in the average distance between friction surfaces which reduces the average magnitude of the normal interaction [11,12]. In the case of longitudinal tangential vibrations, opinion prevails that the decreases in the friction force occur as a consequence of cyclical, instantaneous changes in the vector of the force, taking place in any period of these vibrations when the amplitude of the vibration velocity is greater than that of the sliding motion [16,17,21,25–28]. This phenomenon has been denoted as the "friction vector effect". In the case of transverse vibrations it is generally accepted that decrease in the friction resistance occur as a consequence of changes in direction of the vector of the friction force around the sliding direction separating it into two components: one parallel and one transverse to the direction of motion, and as a consequence only a partial interaction can take place in the direction of the motion [21,25–28].

Micro-vibrations of high frequency, particularly ultrasonic, have been utilised in numerous technological processes associated with mechanical interaction between bodies. Examples include in machining (e.g., in turning or drilling) to reduce frictional forces between the tool and the machined piece, or between the tool and the chip. Considerable gains can be achieved including reduction in power consumption, increases in tool lifetimes as well as an improvement in quality (e.g. smoothness) of the machined surface. In the case of plastic forming the micro-vibrations are utilised for both, minimisation of the external friction—between the tool and the material formed, and for the reduction of the internal friction within the processed material. Wires or tubes can be drawn with multi-fold reduction in the force needed for the actual process simply by including vibrations. Screws can also be tightened with considerably less torque through an instantaneous reduction in the friction forces supplied by micro-vibrations.

Conversely reduction in friction forces, particularly in an uncontrolled manner through vibrations, is not always desirable, e.g. in dismountable joints of machine elements it can lead to loosening of connections (undoing screws or nuts), during a machine's operation, which may ultimately lead to the machine being damaged.

The level of friction reduction in sliding motion under the influence of forced vibrations may vary considerably. There may be no reduction at all, or it may be so large that the value of the friction force in the presence of forced vibrations might be manifold lesser than the actual value of the force in sliding motion carried out without vibrations. It is due to the fact that the magnitude of the change of friction force under the influence of vibrations depends not only on the vibrations parameters such as the frequency and amplitude and their direction, but also on the relative velocity of the motion between the moving object and the support, as well as on contact parameters such as the roughness of surfaces in contact, or the contact rigidity, and others.

Such multitude of factors influencing the ultimate effect of forced vibrations on the friction force leads to the fact that regardless of global interest of many research centres in this topic and regardless of numerous studies dedicated to theoretical analyses and experimental investigation of this subject, until now the mechanism of reduction of the friction force under influence of vibrations is still not yet fully investigated or fully identified. This creates significant difficulties in the conduct of simulational analyses due to their insufficient consistency with experimental results.

One of the reasons for this is the fact that as a rule, in estimations in which friction forces are considered, the simplified, i.e. static friction models based on the Coulomb's model of friction are assumed. In these models deformation in the contact zone of two bodies moving in relation to one another is not taken into account. Significantly better results can be achieved by conducting the analyses using dynamic friction models, such as: the Dahl model [36,37], the LuGre model [38], or the Dupont model [39,40] in which the real elasto-plastic characteristics of the contact are considered.

In this work, through the means of computational analysis carried out with the use of dynamic friction models, the authors undertook the task of explaining the phenomenon of reduction of the drive force needed to initiate a body's sliding motion and required to maintain such motion, under the influence of forced longitudinal tangential vibrations of high frequency. Such effect is frequently described as the reduction of the average friction force.

Simulations were carried out in a Matlab/Simulink environment. The results achieved through computational estimations were compared to experimentally measured data. It is shown that the reduction of the drive force in sliding motion under the influence of forced longitudinal tangential vibrations, identified with the reduction of the average friction force, may take place without a change in the sign of the friction force vector.

2. Experimental investigations and their outcomes

The main objective of experimental investigations presented in this work was to determine quantitative variations in the driving force F_d of a given body during its sliding over support after imposing vibrations to the support in the direction aligned with the realised motion. The second objective was the examination of changes in sliding friction force, F_F, taking place at the contact of the sliding body with the support under the influence of the imposed tangential longitudinal vibrations.

The investigations were conducted using a novel experimental stand specifically designed by the authors of this work. A detailed description of the stand is provided elsewhere [31], however Fig. 1 shows an image of its mechanical part.

The main component is a specifically designed sliding pair whose upper specimen is moved over the ball-bearing supported slide constituting a lower specimen which can be exited into vibrations aligned with direction of the motion of the upper part. The sliding pair has been designed according to finite elements modelling results to ensure that the most uniform achievable

pressure is attained on both interacting surfaces under external loading normal to the contact surface. The overall contact area is 1200 mm^2.

The upper specimen of the sliding pair, in the shape of a rectangular prism, slides over the lower specimen via a system comprising of a linear guide EPX40, a step-motor with a gear box, a driver and a power unit controlling the work of the motor. The entire system is controlled by a computer and MONOPACT LT controller. The lower specimen is excited into high frequency vibrations by a piezoelectric element. The signal is generated and controlled by the DS1104 control & collect card. The driving force is measured by a ring dynamometer. In order to control the transfer of vibrations from the lower to upper specimen, the accelerations of both the bodies are measured. Tests can be conducted under variable normal contact pressure which can be adjusted in a step-wise or continuous mode.

Fig. 2 presents the experimentally determined driving force characteristics in the three following consecutive stages of sliding of an upper part of sliding pair over its lower part, for four measurement variants. All measurements were conducted at a drive velocity v_d=0.62 mm/s. The value of normal pressure has been pre-set at p=0.031 N/mm^2. At each measurement variant, the first and third stage of sliding was conducted without vibrations of the lower specimen whilst the interim, i.e. second stage—under forced harmonic vibrations at a constant frequency f=3900 Hz. In the presented measurement variants the amplitude v_a of the velocity of forced vibrations was equal to 0.20, 1.06, 1.94 and 6.46 mm/s.

It is apparent from the characteristics presented that in the case when amplitude of velocity of forced vibrations is greater than the drive velocity ($v_a > v_d$, in Fig. 2b–d), the excitation of longitudinal tangential vibrations caused a significant decrease in the driving force. Such effects did not occur when $v_a < v_d$ (Fig. 2a). It is seen then that the magnitude of the force reduction, at a given sliding velocity, significantly depends on the amplitude v_a, of the velocity of forced vibrations of the support. The greater such amplitude, in relation to the nominal velocity of sliding of the upper specimen of the sliding pair, the greater is resultant reduction of the driving force.

Based on characteristics determined by varying the magnitude of the amplitudes v_a, of the velocity of forced vibrations at a pre-determined frequency f of such vibrations and at pre-determined nominal drive velocity v_d of the upper specimen and pre-determined contact pressure in the direction normal to the sliding contact it is possible to develop master curves representing the relationship between driving force and amplitude of longitudinal tangential vibrations. Such relationships will be presented in the further part of this work during discussion and verification of the simulating analyses results.

During the investigations, together with measurements of the driving force, changes in acceleration $\ddot{x}$ of the sliding specimen were also measured in the direction of the sliding motion. Consequently, it was possible to determine the profile of the forces of inertia F_i of this specimen ($F_i = -m \cdot \ddot{x}$) at each instance of its movement over the motionless or vibrating support. Knowing the characteristic of the driving force and that of the force of inertia of moving specimen it is possible, utilising the Newton's second law of dynamics, to determine the time-related variability of friction forces acting on the specimen at its surface in contact

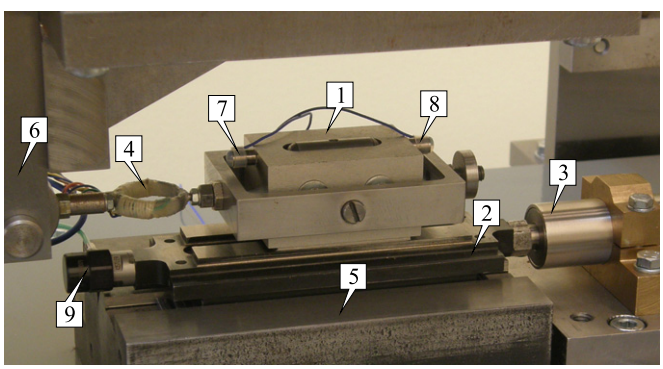

Fig. 1. Photo of the mechanical part of the ready for investigation test rig: 1: upper sample, 2: bottom sample, 3: vibration exciter, 4: ring dynamometer, 5: fixed base, 6: driver, 7–9: accelerometers.

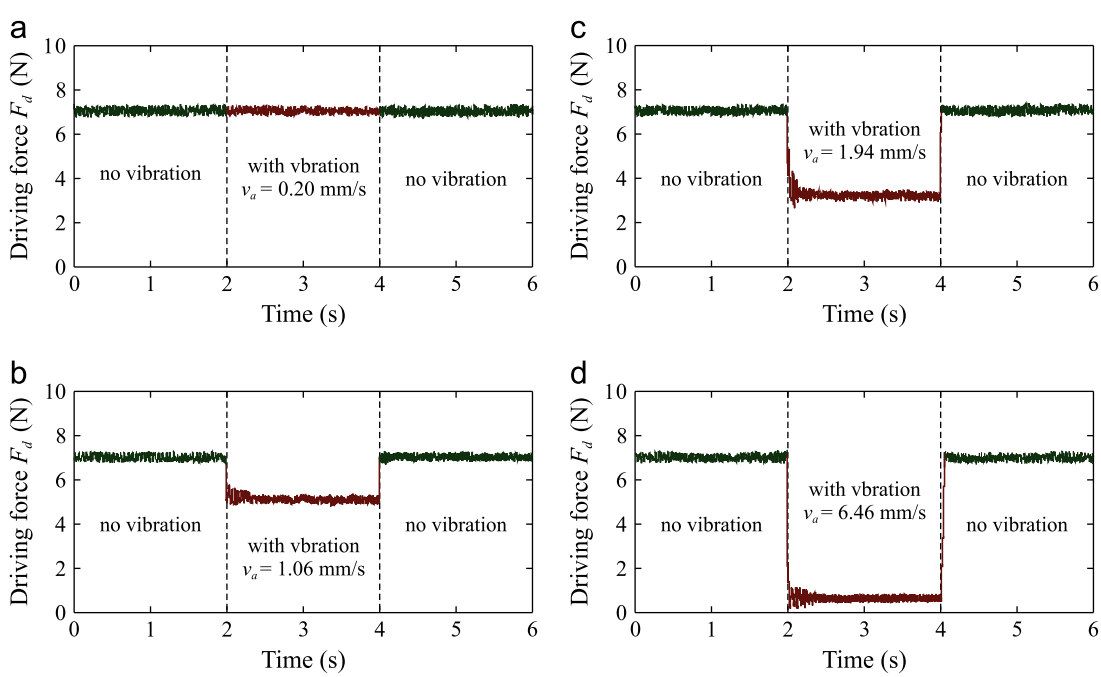

Fig. 2. Profiles of the driving force F_d at drive velocity v_d=0.62 mm/s for various variants of forced vibrations velocity: (a) v_a=0.2 mm/s, (b) v_a=1.06 mm/s, (c) v_a=1.94 mm/s and (d) v_a=6.46 mm/s.

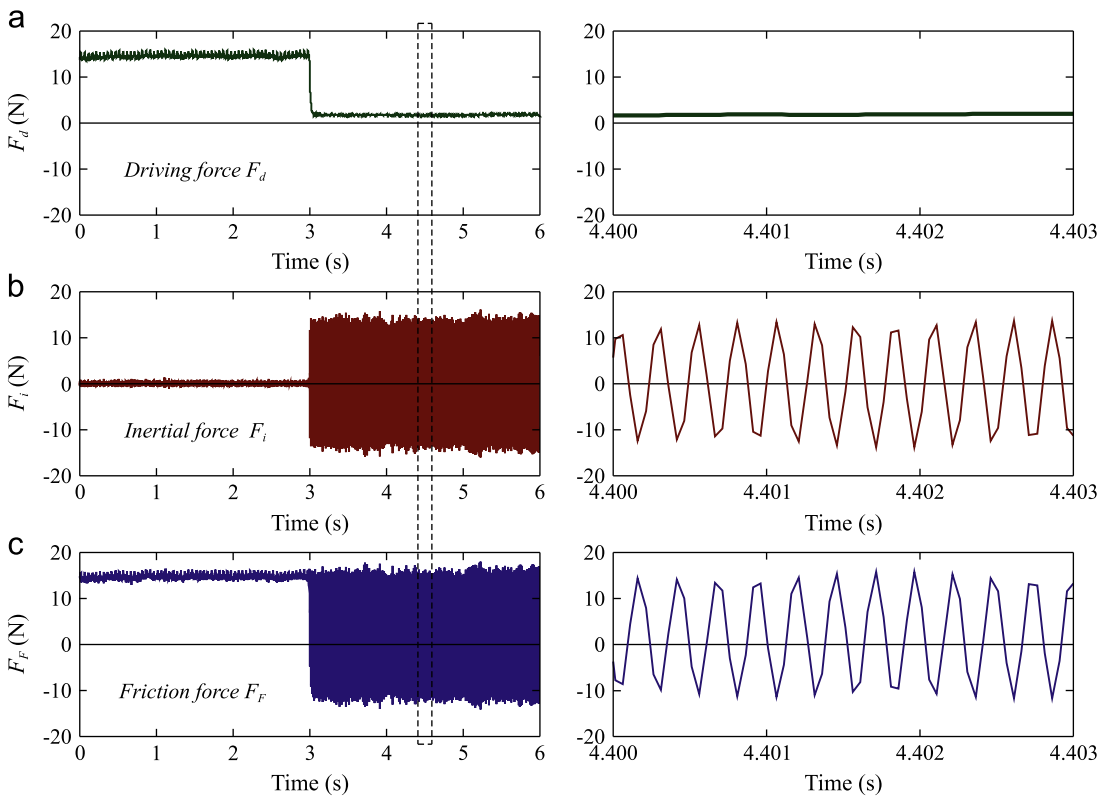

Fig. 3. Experimentally determined characteristics of forces F_d, F_i and F_F during sliding the specimen over the motionless and over the vibrating support; f=3900 Hz, v_a=3.44 mm/s, v_d=0.62 mm/s and p=0.054 N/mm^2.

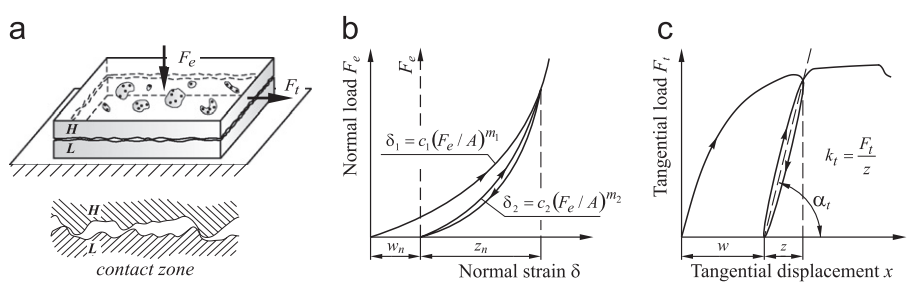

Fig. 4. Elasto-plastic properties of contact: (a) real contact, (b) normal compliance characteristic of contact and (c) shear compliance characteristic.

with the support. Examples of the experimentally determined time characteristics of F_F, F_i and F_d are illustrated in Fig. 3.

The results achieved from experimental investigations were used for the verification of computational procedures elaborated in the Matlab/Simulink environment which facilitated simulating analyses to be carried out regarding the variability of driving force and friction force taking place under the sliding motion of forced longitudinal tangential vibrations.

3. Models and principal mathematical relationships

Three simple models of friction were utilised in the computational procedures developed here. The first of these, treated as a reference, was the classical Coulomb friction model which assumes that the contact zone of the sliding body is non-deformable. It was shown, however, during dynamic analyses, that this model is not sufficiently accurate. Hence, for further investigations two other, so-called dynamic friction models were adopted: the Dahl model [36,37] and the Dupont model [39,40] which, as distinct from the static models are considering the real elasto-plastic properties of the contact zone (Fig. 4), and in particular its tangential contact compliance and the phenomenon of so-called presliding effect.

It has been assumed in the analyses that a body of mass m is moved over the vibrating support through the use of a mechanical drive of known elastic characteristic—the stiffness coefficient k_d of the driving system is known (Fig. 5a). The damping of the system has been assumed to be zero (h_d=0). It has been also assumed that the point B of the attachment of the driving force F_d is moving at the pre-determined speed v_d. The distribution of forces acting upon a sliding body is given in Fig. 5b.

A vector equation of sliding motion of a body moving in a stationary reference system 0xy (Fig. 5) has the following form:

$$m\vec{a} = \vec{F}_d + \vec{F}_g + \vec{F}_e + \vec{F}_F + \vec{F}_N \tag{1}$$

where m is the mass of the body, $\vec{a}$ is the acceleration, $\vec{F}_d$ is the driving force, $\vec{F}_g$ is the force of gravity, $\vec{F}_e$ is the external load perpendicular to the sliding surface, $\vec{F}_F$ is the friction force and $\vec{F}_N$ is the support's normal reaction.

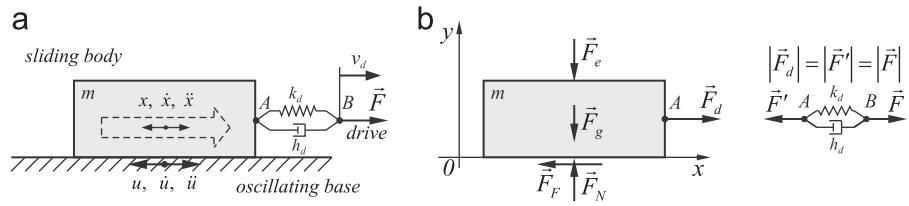

Fig. 5. Model assumed in simulation computations: (a) realisation of sliding motion and vibration excitation and (b) distribution of forces acting on sliding body.

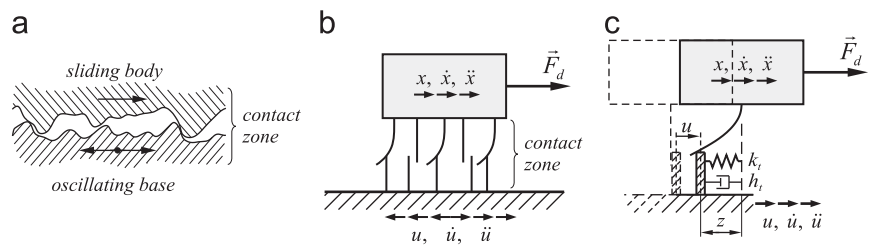

Fig. 6. Modelling of contact zone in Dahl's and Dupont's model of friction: (a) real contact, b) modelling of asperities in contact zone and (c) elastic strain "z" of contact zone in presence of longitudinal vibrations of foundation.

From the above, a scalar equation of this body's motion along the 0x axis is achieved in the following form:

$$m\ddot{x} = F_d - F_F \tag{2}$$

During its motion over the vibrating support the sliding body is also subjected to vibrations as a result of the transfer of vibrations from the support. Consequently, the driving force F_d does not have the constant value. It is a function of a variable, elastic deformation of the drive's components. Assuming a linear characteristic of the elasticity of the driving system, the value of this force is proportional to the magnitude of elastic deformation λ of its components. In the estimated model, the magnitude of this deformation relates to the relative displacement of A and B-ends of an elastic component modelling the drive (Fig. 5).

$$\lambda = x_B - x_A = v_d t - x \tag{3}$$

From the above, the magnitude of driving force can be estimated from the following relationship:

$$F_d = k_d \lambda = k_d(v_d t - x) \tag{4}$$

In the Coulomb model it is assumed that the friction force F_F is described as follows:

$$F_F = \mu F_N \operatorname{sgn}(v_r) \tag{5}$$

where v_r is the relative velocity of sliding body and that of vibrating support and μ is the coefficient of static friction.

The relative velocity v_r of the sliding body in relation to vibrating support equals to the difference of velocity $\dot{x}$ of this body, and velocity $\dot{u}$ of vibrations of the support in the sliding direction x, and hence:

$$v_r = \dot{x} - \dot{u} \tag{6}$$

Eq. (2) of motion of a body over vibrating support in the case of Coulomb static model of friction, after considering relationships (4) and (5) attains the following form:

$$m\ddot{x} = k_d(v_d t - x) - \mu F_N \operatorname{sgn}(v_r) \tag{7}$$

It is assumed in Dahl [36] and Dupont [39] dynamic models of friction that the magnitude of friction force F_F is associated in a real manner with the elastic strain z of the contact measured in the sliding direction (Fig. 6) and is described through the following relationship:

$$F_F = k_t z \tag{8}$$

where k_t is the coefficient of stiffness in the tangential direction, and z is the elastic strain of the contact in sliding direction.

Equation of motion of a sliding body in this case attains the following form:

$$m\ddot{x} = k_d(v_d t - x) - k_t z \tag{9}$$

In Dahl and Dupont models it is assumed then that a relationship exists between the velocity of elastic deformation of the contact $\dot{z} = dz/dt$ and the relative velocity v_r of sliding body in relation to the support. This relationship, in the case of Dahl model, is expressed as follows [36]:

$$\dot{z} = \frac{dz}{dt} = v_r\left[1 - \frac{k_t}{\mu F_N}\operatorname{sgn}(v_r) z\right]^a \tag{10}$$

whilst in the case of Dupont model, by the following relationship [39]:

$$\dot{z} = \frac{dz}{dt} = v_r\left[1 - \beta(z, v_r)\frac{k_t}{\mu F_N}\operatorname{sgn}(v_r) z\right]^a \tag{11}$$

where α is the parameter determining the shape of relationship between tangential displacements and tangential force. Bliman [41] states that for brittle type materials the magnitude of this parameter is in the region of $0 \le \alpha < 1$ whilst for ductile type materials $\alpha \ge 1$. The method for determining the $\beta(z, v_r)$ function in consecutive stages of tangential displacements is described in work [39].

In simulating computations it has been assumed that vibrating motion is harmonic and has the following form:

$$u = u_0 \sin(\omega t) \tag{12}$$

where u_0 is the amplitude of forced vibrations, whilst $\omega = 2\pi f$, where in turn f is the vibrations frequency.

Hence, the velocity of forced vibrations is described by the equation:

$$\dot{u} = u_0 \omega \cos(\omega t) \tag{13}$$

where the product $u_0\omega$ is the amplitude of the velocity v_a of these vibrations, and hence:

$$v_a = u_0\omega = 2\pi f u_0 \tag{14}$$

4. Simulating analyses

Utilising relationships (2)–(14), a computational model has been developed in the Matlab/Simulink environment, which has been used for numerical analysis of the influence of tangential contact vibrations on the drive force and friction force in the presence of forced longitudinal tangential vibrations. Examples of computations are presented as master curve characteristics in Figs. 7–14.

Fig. 7 illustrates the time characteristics of displacements x_A and velocity v_A of the sliding body, the characteristics of drive velocity v_d, velocity of the vibrating support v_v and the relative velocity v_r as well as time characteristics of the friction force F_F determined for the Dahl and Coulomb models. These diagrams are generated in those cases when the amplitude v_a of vibrations velocity is less than the drive velocity v_d. Figs. 8 and 9, in turn, illustrate corresponding characteristics for those cases when the amplitude of vibrations velocity is greater than the drive velocity.

It can be seen from the presented results that in the case of sliding motion proceeding under forced longitudinal tangential vibrations at the velocity amplitude v_a less (or equal) than the drive velocity v_d, the computed values of friction forces do not depend on the assumed friction model. The friction force during sliding retains a constant value $F_F = \mu F_N = const$, which means that under such conditions the forced vibrations do not influence its time runs.

A completely different situation is observed when the amplitude of velocity of forced longitudinal tangential vibrations is greater than the drive velocity ($v_a > v_d$). It appears that in such a case the friction force does not retain constant value during sliding of a given body over vibrating support, but undergoes cyclic changes. Simultaneously, the results of computations clearly depend on the friction model assumed. For the Coulomb model, each change of the sign of relative velocity v_r of sliding motion caused by the forced vibrations is associated with the immediate change of the sign of friction force vector whilst an absolute value of this force remains unchanged.

The results of friction force computations carried out with the use of dynamic friction models such as the Dahl, Dupont or LuGre models show that a change of the friction force profile in the presence of longitudinal, tangential contact vibrations is not stepwise, when condition $v_a > v_d$ is satisfied, but rather continuous. At small differences between v_a and v_d, after the relative velocity attains a zero-value (i.e. after v_r drops to zero) the instantaneous magnitude of the friction force is gradually reduced to the minimum value but without the change of sign (Fig. 8c). The minimum value of the friction force is achieved at the moment of consecutive passing of relative velocity through the zero-magnitude, after which the friction force starts to gradually increase.

At large differences between v_a and v_d, after the drop of relative velocity to zero, the instantaneous magnitude of friction force starts to gradually reduce to zero, after which a change of its sign takes place associated with its increase in the opposite direction (Fig. 9c). After attaining the maximum magnitude (with a changed sign, however) which takes place at a consecutive zeroing of relative velocity (v_r=0), a gradual decrease of the friction force commences, followed by the passing through zero and then, its gradual increase to the maximum value; the latter is attained at a consecutive change of relative velocity sign (v_r) i.e. during a consecutive drop of relative velocity to zero.

The described changes take place cyclically during each period of vibrations. They are a consequence of cyclic changes in the magnitude and direction of elastic deformations of roughness

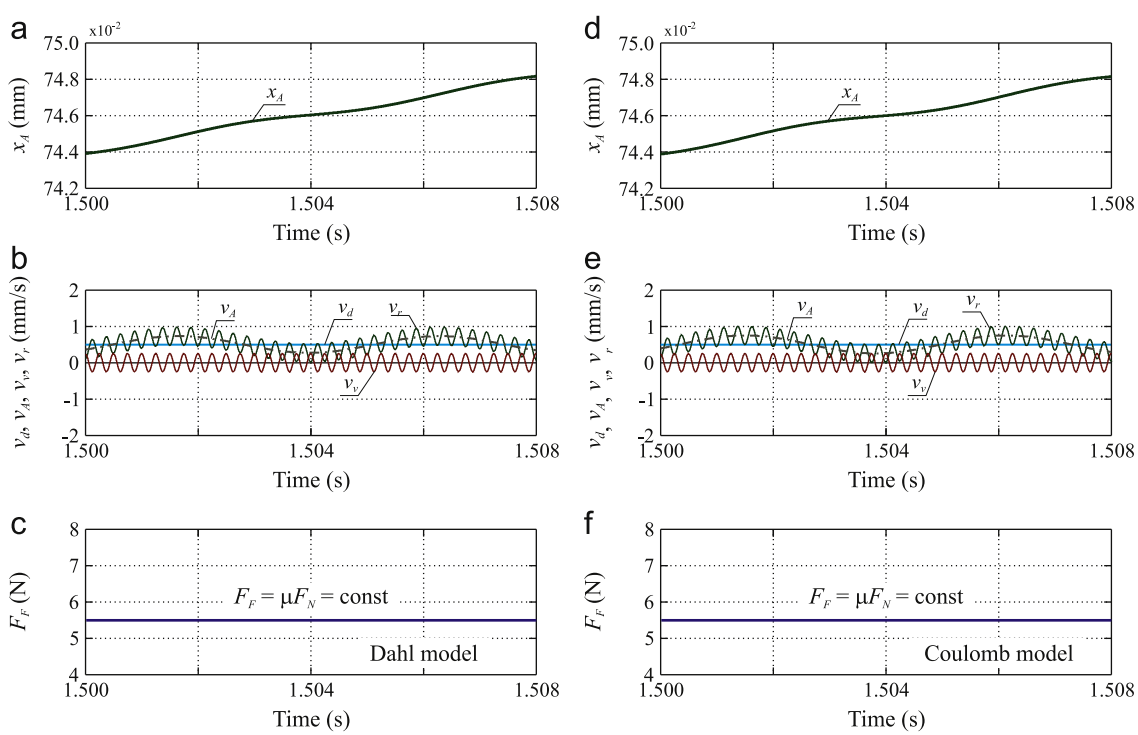

Fig. 7. Time characteristics of x_A, v_A, v_v, v_r and friction force F_F determined at the frequency f=4000 Hz, when v_a=0.25 mm/s < v_d=0.5 mm/s; (a–c) Dahl model, (d–f) Coulomb model.

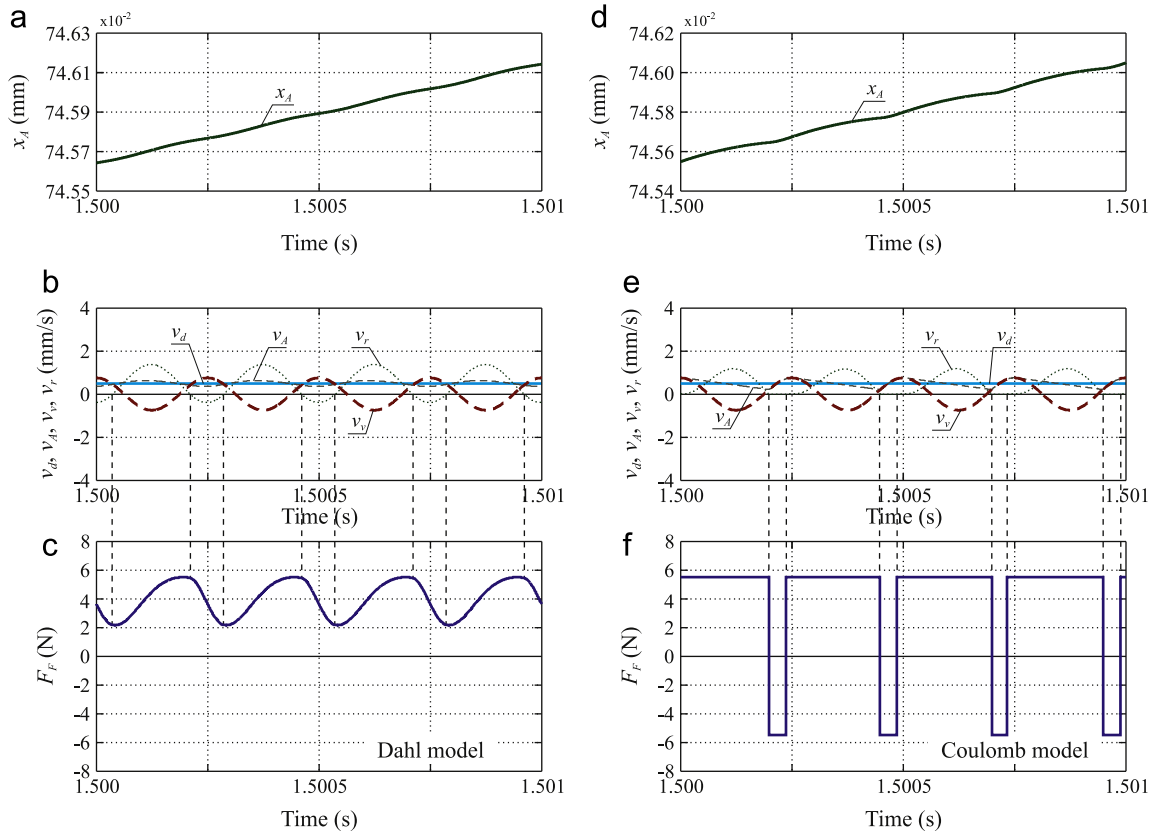

Fig. 8. Time characteristics of x_A, v_A, v_v, v_r and friction force F_F determined at the frequency f=4000 Hz, when v_a=0.75 mm/s > v_d=0.5 mm/s; (a–c) Dahl model and (d–f) Coulomb model.

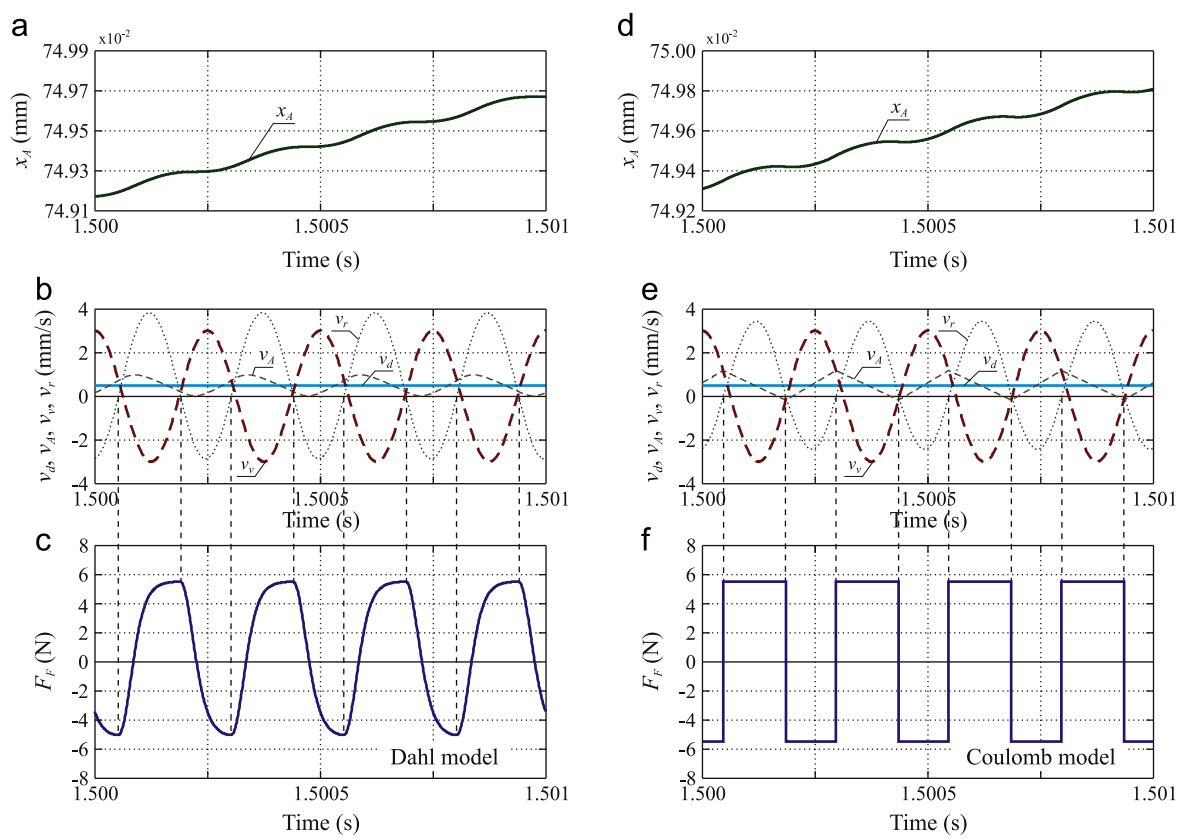

Fig. 9. Time characteristics of x_A, v_A, v_v, v_r and friction force F_F determined at the frequency f=4000 Hz, when v_a=3.0 mm/s > v_d=0.5 mm/s; (a–c) Dahl model and (d–f) Coulomb model.

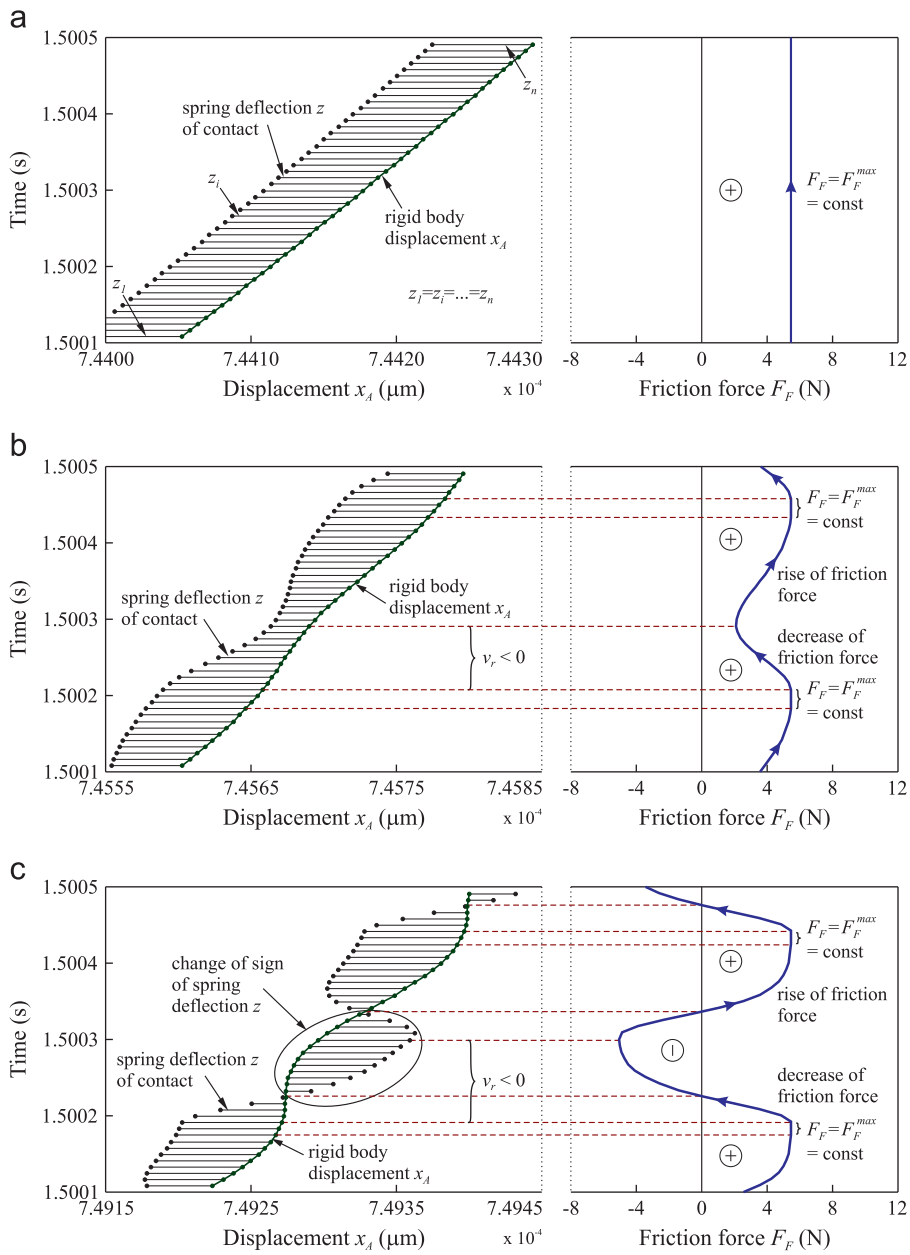

Fig. 10. Graphic representation of changes in friction force F_F in relation to elastic deformation of roughness asperities for the Dahl model; (a) $v_a=0.25$ mm/s $<v_d=0.5$ mm/s, (b) $v_a=0.75$ mm/s $>v_d=0.5$ mm/s and (c) $v_a=3.0$ mm/s $>v_d=0.5$ mm/s.

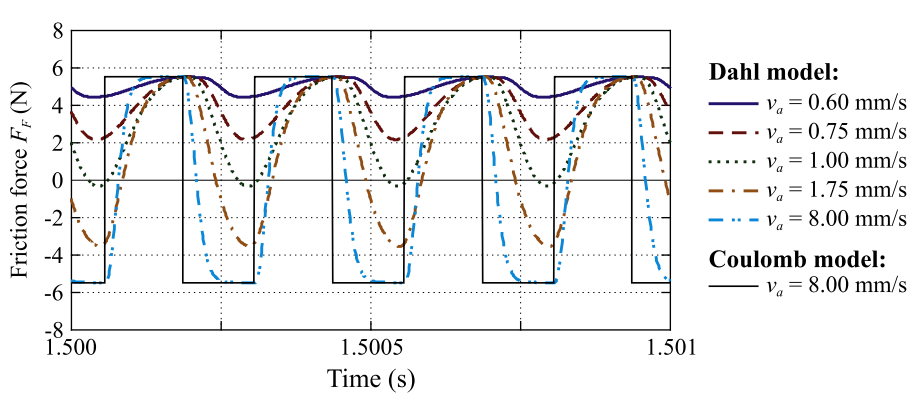

Fig. 11. Time characteristics of the friction force F_F for various amplitudes of vibrations velocity v_a; $f=4000$ Hz, $v_d=0.5$ mm/s and $k_t=80.0$ N/μm

asperities in relation to the path of the sliding body. This phenomenon has been illustrated in Fig. 10.

Fig. 11 illustrates examples of friction force profiles F_F determined with the use of Dahl model at drive velocity v_d=0.5 mm/s and the force frequency f=4000 Hz for five magnitudes of vibrations velocity amplitude v_a=0.60, 0.75, 1.0, 1.75 and 8.0 mm/s.

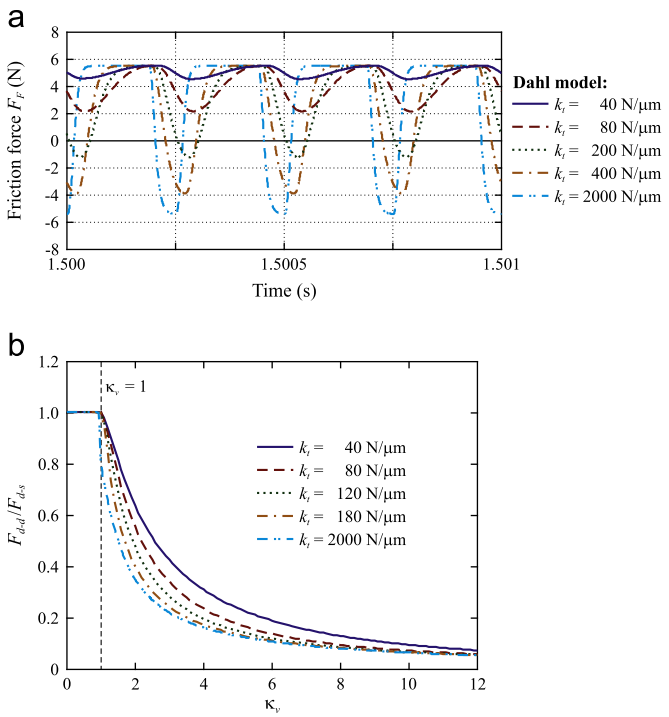

Fig. 12. Influence of the contact stiffness on: (a) profile of friction force F_F, (b) reduction of the drive force F_d in the presence of longitudinal tangential vibrations; f=4000 Hz, v_a=75 mm/s, v_d=0.5 mm/s; Dahl model.

Computations were carried out assuming that the coefficient of tangential stiffness of the contact area, k_t=80.0 N/μm. This particular value has not been selected randomly. In experiments carried out with the view of verification of simulating analyses, the sliding pairs were used for which the surface roughness R_a=0.26 μm (for the upper, steel specimen) and R_a=0.35 μm (for the lower, cast iron specimen). Experiments targeting determination of dry contact stiffness for such sliding pairs [34] under normal pressures identical to those utilised during simulating analyses, i.e. p=0.046 N/mm^2 yielded the given above value of the tangential stiffness coefficient of the contact analysed. For comparison, Fig. 11 illustrates also the profile of friction force for the Coulomb model determined at the drive velocity v_d=0.5 mm/s and the forced vibrations velocity amplitude v_a=8.0 mm/s.

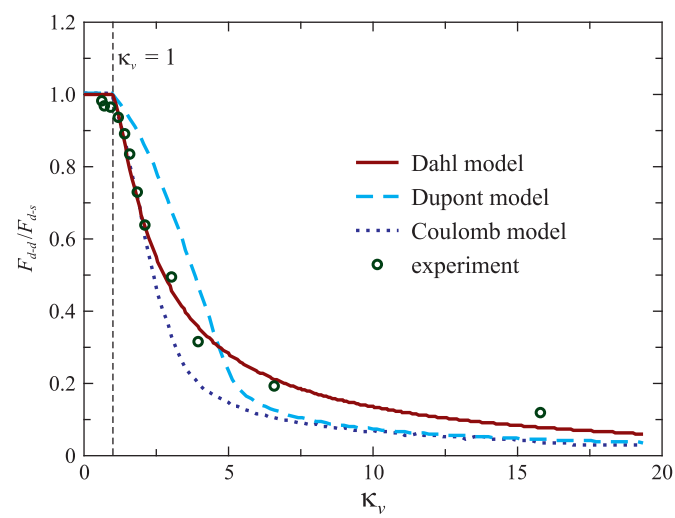

Fig. 14. Comparison of computed changes of the drive force F_d under the influence of longitudinal tangential vibrations with results of experiments.

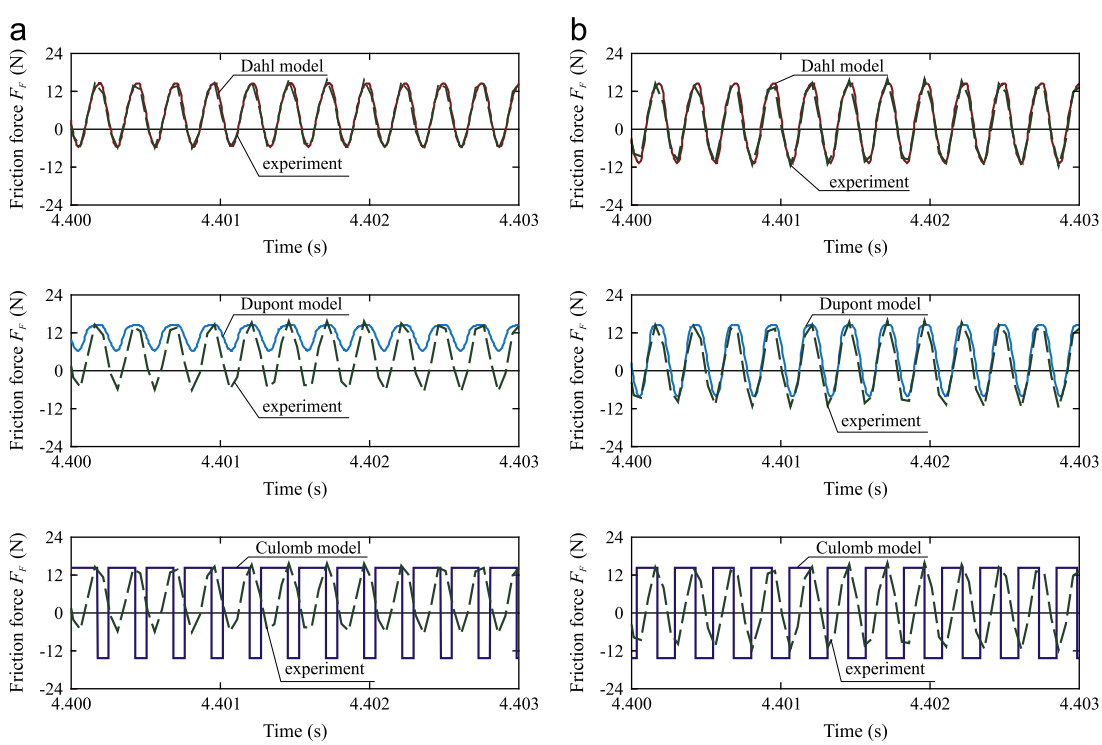

Fig. 13. Comparison of computed runs of friction force F_F for various friction models with results of experiments: (a) v_d=0.62 mm/s and v_a=1.76 mm/s, (b) v_d=0.62 mm/s and v_a=3.44 mm/s.

In the Dahl, Dupont and LuGre dynamic models the friction force is a function of the contact stiffness in the tangential direction, whose measure is the coefficient of stiffness k_t. Fig. 12a presents the profiles of this force, computed with the use of Dahl model, for selected values of k_t, at frequency of excitation $f=4000$ Hz and the vibrations velocity amplitude $v_a=0.75$ mm/s. It was assumed in computations that $v_d=0.5$ mm/s. Fig. 12b, in turn, presents graphs of $F_{d-v}/F_{d-s}=f(\kappa_v)$ generated for the same values of k_t which illustrate a profile of variability of drive force F_{d-v} under the influence of forced longitudinal, tangential vibrations in relation to the magnitude of F_{d-s} of this force without vibrations as a function of a dimensionless coefficient $\kappa_v=v_a/v_d$.

It can be seen from these graphs how important the tangential contact stiffness is on the friction force and on the magnitude of drive force variability in sliding motion in the presence of longitudinal tangential vibrations. Assuming an erroneous value of the coefficient of tangential stiffness k_t i.e. different than that in a real contact, may lead to significant errors and lack of compliance between the computational and experimental results. It can also be seen from the graphs in Fig. 12b that in each case when the coefficient κ_v attains the value greater than 1, which refers to the fulfillment of the requirement of the amplitude v_a of forced vibrations velocity being greater than the nominal drive velocity v_d ($v_a > v_d$), the drive force is reduced. At a sufficiently high value of coefficient κ_v it is possible to achieve a greater than 20-fold reduction of the drive force essential to initiate sliding motion of a body and to maintain this motion.

5. Experimental verification of computational analyses results

The results of computational analyses were verified through their comparison with the outcomes of experiments carried out on the test stand described earlier. Fig. 13 illustrates a comparative example of time characteristics of friction force generated through simulating analyses, carried out using three friction models (Dahl, Dupont and Coulomb) analysed in this paper, in relation to experimental results. The comparison is presented for a steel/steel frictional couple for two individual sets of input data. It has been assumed in both cases that the velocity amplitude v_a of forced vibrations is greater than the nominal drive velocity $v_d=0.62$ mm/s. For the first set, $v_a=1.76$ mm/s has been assumed, whilst for the second set, $v_a=3.44$ mm/s. Experiments were conducted for dry contacts at the input frequency $f=3900$ Hz. The mass of the moving body was $m=0.5$ kg, whilst the nominal surface of the body contact with the support was $S=1200$ mm^2. Roughness parameter R_a of the contact surface was $R_a=1.01$ μm for the support, whilst for the moving body, $R_a=0.26$ μm. Additional external load on the sliding body in the direction perpendicular to the movement was $F_e=61.8$ N. Stresses normal to the contact surface in the case analysed were $p=0.056$ N/mm^2. The experimentally determined value of the coefficient of tangential contact stiffness of the contact under investigation was $k_t=78$ N/μm. The measurements of this coefficient were conducted using a stand described in work [34].

Fig. 14 illustrates a comparison of the computationally determined changes of the drive force, F_d, under the influence of longitudinal tangential vibrations with that achieved experimentally. The investigations were carried out for dry contacts at the forced frequency $f=2600$ Hz. The nominal drive velocity was $v_d=0.31$ mm/s, external load $F_e=31.8$ N, $p=0.031$ N/mm^2 and $k_t=72$ N/μm. A variability of amplitude v_a of the vibrations velocity was achieved by varying the amplitude u_0 of these vibrations.

It can be seen from the comparison presented in Figs. 13 and 14 that analyses carried out with the use of Dahl friction model yield a very good agreement between simulated computations and experimental results. No such agreement was achieved when Coulomb or Dupont models were used.

6. Summary

Both simulation and experimentally measured data clearly demonstrate that the effect of reduction of driving force essential for initiating and for continuing sliding motion is observed both at high- and at low-frequency vibrations, whilst the criterion for its occurrence is the requirement that the amplitude v_a of the vibrations velocity is greater than the drive velocity v_d ($v_a > v_d$).

At an imposed nominal velocity of sliding of a given body over the vibrating support the reduction of this force can be controlled through an appropriate selection of vibrations frequency and/or their amplitude due to the fact that the amplitude of vibrations velocity is a function of these two factors.

However, the consideration of only vibration factors (amplitude and frequency) and nominal sliding velocity during computations of the drive force, essential for initiating and maintaining the sliding motion in the presence of longitudinal tangential vibrations, is not sufficient because this force also depends substantially on the tangential stiffness of the contact which, in turn, is a function of normal stresses and the contact's surface roughness. Assuming an inappropriate value of the contact tangential stiffness coefficient always results in an erroneous value of estimation of this force. In extreme cases, the computational error can exceed the true value of the drive force by more than 100%.

It has been shown in this work that the commonly accepted view that the reduction of the drive force in sliding motion under the influence of forced longitudinal tangential vibrations, is a consequence of cyclic changes in the sign of the vector of friction forces taking place in each vibrations period when only the amplitude of the vibrations velocity is greater than the velocity of the sliding motion, is untrue. Such view has resulted from the use of Coulomb frictional models in computational analyses. Computations carried out with the use of dynamic models demonstrate that the phenomenon of reduction of the drive force may take place also without a change in the sign of the friction force vector.

It was found that the best consistency of computational results with experimentally measured data was achieved with the use of the Dahl model of friction. It needs to be emphasised, however, that the analyses presented in this work were carried out at relatively low normal pressure ($p=0.031$–0.081 N/mm^2). At such low pressure, a non-linear dependence of tangential deformations of the contact upon tangential stresses may occur at the initial stages of loading of the contact in the tangential direction, as assumed in the Dahl model. Under higher normal pressure, in the initial stages of application of the tangential stresses the tangential deformations of the contact may be linearly dependent on these stresses and under such circumstances an improvement in the extent of consistence needs to be anticipated between computational analyses carried out with the use of the Dupont model with the experimental results, whilst making agreement with the Dahl model somewhat worse.

References

[1] Baker HD, Claypoole W, Fuller DD. Proceedings of the First US National Congress of Applied Mechanics 1952:23.
[2] Fridman HD, Levesque P. Reduction of static friction by sonic vibrations. Journal of Applied Physics 1959;30:1572–5.

[3] Urbakh M, Klafter J, Gourdon D, Israelachvili J. The nonlinear nature of friction. Nature 2004;430(29):525–8.
[4] Gnecco E, Socoliuc A, Maier S, Gessler J, Glatzel T, Baratoff A, et al. Dynamic superlubricity on insulating and conductive surfaces in ultra-high vaccum and ambient environment. Nanotechnology 2009;20:025501.
[5] Behme G, Hesjedal T. Influence of ultrasonic surface acoustic waves on local friction studied by lateral force microscopy. Applied Physics A 2000;70: 361–3.
[6] Hesjedal T, Behme G. The orign of ultrasound—induced friction reduction in microscopic mechanical contacts. IEEE Transactions on Ultrasonics, Ferroelectrics and Frequency Control 2002;49(3):356–4.
[7] Socoliuc A, Bennewitz R, Gnecco E, Meyer E. Physics Review Letter 2004;92(1):134301.
[8] Socoliuc A, Gnecco E, Maier S, Pfeiffer O, Baratoff A, Bennewitz R, et al. Atomic-scale control of friction by actuation of nanometer-sized contacts. Science 2006;313(14):207–10.
[9] Pohlman R, Lehfeld E. Influence of ultrasonic vibrations on metallic friction. Ultrasonics 1966;4:178–85.
[10] Godfrey D. Vibration reduces metal to metal contact causes an apparent reduction in friction. ASLE Transactions 1967;10:183–92.
[11] Hess DP, Soom A. Normal vibrations and friction under harmonic loads: part I—Hertzian contacts. Journal of Tribology 1971;113:80–6.
[12] Tolstoi DM, Borisova GA, Grigorova SR. Friction regulation by perpendicular oscillation. Soviet Physics—Doklady 1973;17(9):907–9.
[13] Budanov BV, Kudinov VA, Tolstoi DM. Interaction of friction and vibration. Soviet Journal of Friction and Wear 1980;1:79–89.
[14] Grudziński K, Kostek R. Influence of normal micro-vibrations in contact on sliding motion of solid body. Journal of Theoretical and Applied Mechanics 2005;43(1):37–49.
[15] Qu JJ, Zhau NN, Wang YL. Experimental study of air squeeze effect on high frequency friction contact. Tribology International 2010;43:2190–5.
[16] Mitskevich AM. Motion of the body over tangentially vibrating surface, taking account of friction. Soviet Physics—Acoustics 1968;13(3):343–51.
[17] Skare T, Stahl JE. Static and dynamic friction processes under the influence of external vibrations. Wear 1992;154:177–92.
[18] Katoh K. Active control of friction using ultrasonic vibration. Japanese Journal of Tribology 1993;38:1019–25.
[19] Sase N, et al. Reduction of friction without lubrication. Proceedings of the International Conference on AMPT'95 1995;3:1298–304.
[20] Sase N, et al. Control of friction coefficient between metal surfaces. Proceedings of the International Conference on AMPT'97 1997;2:609–15.
[21] Mutuonga Onoda. New gravity compensation method by dither for low-g simulation. Journal of Spacekraft and Rockets 1995;32(2):364–9.
[22] Siegert K, Ulmer J. Reduction of sliding friction by ultrasonic waves. Production Engineering 1998;5(1):9–12.
[23] Siegert K, Ulmer J. Superimposing ultrasonic waves on the dies in tube and wire drawing. Journal of Engineering Materials and Technology 2001; 123:517–23.
[24] Kutomi H, Sase N, Fujii M. Development of friction controller. Proceedings of the International Conference on AMPT'99 1999;1:605–12.
[25] Littmann W, Stork H, Wallaschek J. Sliding friction in the presence of ultrasonic oscillations: superposition of longitudinal oscillations. Archive of Applied Mechanics 2001;71:549–54.
[26] Littmann W, Stork H, Wallaschek J. Reduction of friction using piezoelectrically excited ultrasonic vibrations. Proceedings of the SPIE's 8th Annual International Symposium on Smart Structures and Material. Billingham, Washington; 2001:302–11.
[27] Stork H, Littmann W, Wallaschek J, Mracek M. The effect of friction reduction in presence of ultrasonic vibrations and its relevance to travelling wave ultrasonic motors. Ultrasonics 2002;40:379–83.
[28] Kumar VC, Hutchings IM. Reduction of sliding friction of metals by the application of longitudinal or transverse ultrasonic vibration. Tribology International 2004;37:833–40.
[29] Tsai CC, Tseng CH. The effect of friction reduction in presence of in-plane vibrations. Archive of Applied Mechanics 2006;75:164–76.
[30] Leus M, Gutowski P. The analysis of longitudinal tangential contact vibration effect on friction force using Coulomb and Dahl models. Journal of Theoretical and Applied Mechanics 2008;46(1):171–84.
[31] Gutowski P, Leus M, Parus A. Experimental tests of the influence of the longitudinal tangential contact vibrations on the friction force. Modelowanie Inżynierskie 2008;35(4):39–44 [in Polish].
[32] Gutowski P, Leus M. Reduction of driving force in sliding motion, as an effect of longitudinal tangential vibrations. Tribologia 2009;228(6):13–27 [in Polish].
[33] Leus M, Gutowski P, Parus A. Experimental tests and modelling the longitudinal tangential vibration effect on driving force in sliding motion. Archiwum Technologii Maszyn i Automatyzacji 2009;29(4):127–37 [in Polish].
[34] Leus M, Gutowski P. The influence of tangential stiffness of the contact on friction force in the presence of longitudinal vibrations. Tribologia 2010;232(4):301–11 [in Polish].
[35] Popov VL, Stracevic J, Filipov AE. Influence of ultrasonic in-plane oscillations on static and sliding friction and intrinsic length scale of dry friction processes. Tribology Letters 2010;39:25–30.
[36] Dahl P Solid friction model. Technical Report TOR-0158H3107-181-1. The Aerospace Corporation, El Segundo, CA; 1968.
[37] Dahl P. Solid friction damping of mechanical vibrations. AIAA Journal 1976;14(12):1675–82.
[38] Canudas de Wit C, Olsson H, Astrom KJ, Lischynsky P. A new model for control of systems with friction. IEEE Transactions of Automatic Control 1995;40(3):419–25.
[39] Dupont P, Armstrong B, Heyward V. Elasto-plastic model contact compliance and stiction. Proceedings of the American Control Conference, AACC. Chicago; 2000: pp. 1072–1077.
[40] Dupont P, et al. Single state elasto-plastic friction models. IEEE Transactions of Automatic Control 2002;47(5):787–92.
[41] Bliman PA. Mathematical study of the Dahl's friction model. European Journal of Mechanics A: Solids 1992;11(66):835–48.